

1 **Effects of feedbacks on the climate sensitivity to land cover and CO<sub>2</sub> change in a**  
2 **GCM**

3 M.K. van der Molen<sup>1,2,\*</sup>, B.J.J.M. van den Hurk<sup>1</sup> and W. Hazeleger<sup>1</sup>

4 26 March 2009

5 <sup>1</sup> Royal Netherlands Meteorological Institute (KNMI), PO Box 201, 3730 AE De  
6 Bilt, The Netherlands

7 <sup>2</sup> Now at VU-University Amsterdam, Faculty of Earth and Life Sciences, De  
8 Boelelaan 1085, 1081 HV Amsterdam, The Netherlands

9 \* corresponding author, email: [michiel.van.der.molen@falw.vu.nl](mailto:michiel.van.der.molen@falw.vu.nl)

10

11 Manuscript for submission to Journal of Climate

1 **Abstract**

2 Since the start of the industrial era, land cover change and atmospheric CO<sub>2</sub>  
3 concentration have both changed the radiation budget of the Earth. Land cover  
4 change, mainly deforestation, has a large negative radiative effect through albedo,  
5 which acts locally and during daylight. Increasing CO<sub>2</sub> concentration has a relatively  
6 small positive radiative effect, which however acts continuously all over the world.  
7 Feedbacks modulate the general radiative effects: land cover change causes changes  
8 in energy partitioning and cloud cover, and the warming due to rising CO<sub>2</sub>  
9 concentration causes changes in the general circulation via acceleration of the  
10 hydrological cycle. In the context of the “Land Use Change, IDentification of Robust  
11 impacts” (LUCID) project, the EC-Earth climate model has been used to determine  
12 and quantify those feedbacks. In EC-Earth cooling due to deforestation has a positive  
13 feedback via cloud cover in the tropics and a negative feedback via surface  
14 temperature in the mid-latitudes. Warming due to increased CO<sub>2</sub> concentration has a  
15 positive albedo feedback via melting of snow and ice, the water vapour/lapse rate  
16 feedback and it also intensifies tropical deep convection with mixed long wave and  
17 shortwave feedbacks via changes in cloud cover. Overall, the increased CO<sub>2</sub>  
18 concentration has a warming effect on the majority of the globe, with amplification  
19 towards the poles. Extensive land cover change, notably Central North America and  
20 Eastern Europe, has a stronger cooling effect. The EC-Earth version we use has  
21 prescribed, monthly and annually variable SST’s (i.e. uncoupled ocean model). The  
22 implication of this setup is discussed.

1 **1. Introduction**

2 Land cover and greenhouse gas concentrations have changed simultaneously due to  
3 anthropogenic activity since the industrial revolution. From 1750 to 1992, the fraction  
4 of low vegetation on land has increased from 0.33 to 0.47. The corresponding increase  
5 in albedo has a negative radiative forcing (Forster et al., 2007). The concentration of  
6 CO<sub>2</sub>, the most important greenhouse gas after water vapour, has increased from about  
7 280 ppm in 1700 to 288 ppm in 1870, 356 ppm in 1992 and 386 ppm in 2008 (Tans,  
8 2009), and has a positive radiative forcing. Distinguishing the relative contribution of  
9 land cover change and CO<sub>2</sub> concentration to climate change in historic times is  
10 important to understand the climate dynamics and to improve our capability to project  
11 anthropogenic influence on future climate. It is also relevant, because both CO<sub>2</sub>  
12 emissions and land cover change are continuing at unprecedented rates.

13

14 The concept of radiative forcing has been used often to compare the response of the  
15 Earth radiative energy balance to different external forcings. Ramaswamy et al (2001)  
16 define radiative forcing as the change of the net (shortwave and long wave) radiation  
17 at the tropopause after adjustment of stratospheric temperatures to radiative  
18 equilibrium. Relatively simple conceptual models such as Radiative Convective  
19 Models (e.g. Manabe and Strickler, 1964) are useful tools for deriving estimates of the  
20 radiative forcing of a range of perturbations. However, comparing the radiative  
21 forcing of for instance land cover change and changes in the CO<sub>2</sub> concentrations may  
22 conceal important feedbacks that lead to different responses of the climate system to  
23 these forcings. We note that the enhanced greenhouse effect acts continuously and  
24 over the entire surface of the Earth. The land use related albedo effect acts locally  
25 where the land cover has changed and only during day time. It is thus likely that in

1 deforested regions and during daylight the albedo effect exceeds the enhanced  
2 greenhouse effect. Furthermore, land cover change is through albedo intimately linked  
3 with energy partitioning at the surface and has therefore a great potential to actively  
4 change boundary layer processes. Similarly, increasing CO<sub>2</sub> concentrations do not  
5 only change the long wave radiation budget, but may also impact the hydrological  
6 cycle, which is closely linked to the water vapour concentration, clouds and the  
7 atmospheric lapse rate (Bony et al., 2006, Davin et al., 2007, Dessler and Sherwood,  
8 2009). Another example is demonstrated by the impact of clouds on the radiation  
9 budget, which is large relative to  $\Delta RF_{lcc}$  and  $\Delta RF_{CO_2}$ . The presence of clouds is  
10 connected with the surface fluxes of water vapour and sensible heat: the first provides  
11 the moisture and the second the vertical mixing needed for cloud formation. As such,  
12 changes in cloud formation may form an important feedback to land cover change and  
13 rising CO<sub>2</sub> levels. These are examples of feedback mechanisms that are not readily  
14 incorporated in first order estimates of the radiative forcing as defined above. The  
15 presence of such feedbacks makes the use of complex earth system/climate models  
16 inevitable.

17  
18 A number of studies have used global circulation models (GCMs) of land cover  
19 change, some focussed on the tropics (Polcher and Laval, 1994, McGuffie et al., 1995,  
20 Zhang et al., 1996a,b) and some on the global changes (Zhao et al., 2001, Bounoua et  
21 al., 2002, Matthews et al., 2004, Feddema et al., 2005). Other studies focussed on the  
22 effect of rising CO<sub>2</sub> levels (Cox et al., 2000, Friedlingstein et al., 2003). However,  
23 studies of the relative radiative forcing of simultaneous land cover change and CO<sub>2</sub>  
24 levels are few (*cf.* Pitman and Zhao, 2000, Brovkin et al., 2004, Davin et al., 2007).

25

1 It is the objective of this paper to study how the initial effect of changes in land cover  
2 and CO<sub>2</sub> concentration on climate are modified by additional feedbacks, how these  
3 feedbacks differ between the two types of forcing, and how they vary regionally. We  
4 employ a Radiative Convective Model (Van Dorland, 1999) to estimate the radiative  
5 forcing of both land cover change and elevations in the global mean CO<sub>2</sub>  
6 concentration between 1750, 1870 and 1992. This RCM approach gives an adequate  
7 estimate of the radiative forcing of land cover change and increasing CO<sub>2</sub>  
8 concentration, when the surface and tropospheric state are held fixed. We also assume  
9 that both impacts are linearly additive. Calculations with the GCM allow an  
10 assessment of the net effect including all feedbacks, and the difference between GCM  
11 results and the RCM estimate is used to calculate the feedback strength.

12

## 13 **2. Methods**

### 14 *a. Radiative-Convective Model Calculations*

15 Concerning land cover change, Table 1 indicates the albedo of different surface types  
16 and their relative distribution over the Earth in 1750, 1870 and 1992. In the absence of  
17 clouds and aerosols, the albedo is estimated to be 0.1079 in 1750, 0.1087 in 1870 and  
18 0.1102 in 1992. The (change in) radiative forcing due to land cover change between  
19 1870 and 1992 ( $RF_{lcc}$ ) is calculated using a Radiative Convective Model (RCM) by  
20 evaluating the tropopause net shortwave radiation response to the change in surface  
21 albedo. The RCM (Van Dorland, 1999) used in this study is largely based on the  
22 original concepts of Manabe and Strickler (1964) and Manabe and Wetherald (1967).  
23 In the RCM clouds were specified at three levels (representing low, mid and high  
24 clouds) and kept constant during the calculations. The tropopause was defined as a  
25 fixed height (179 hPa) and also unchanged. By this procedure the change in  $RF_{lcc}$

1 between 1870 and 1992 was estimated to be  $-0.19 \text{ W m}^{-2}$  (Table 2). The  $\text{RF}_{\text{lcc}}$  is  
2 within the range of  $-0.2 \pm 0.2 \text{ W m}^{-2}$  between 1750 and 1990 given by IPCC (Forster  
3 et al., 2007), Betts et al. (2001, 2007) and Hansen et al. (1998). The  $\text{RF}_{\text{lcc}} = -0.19 \text{ W}$   
4  $\text{m}^{-2}$  represents the radiative forcing at the tropopause, after stratospheric adjustment,  
5 which is commonly used for  $\text{CO}_2$  (IPCC, Shine et al., 1995). In a similar manner, the  
6 radiative forcing due to the increasing  $\text{CO}_2$  concentrations ( $\text{RF}_{\text{CO}_2}$ ) was estimated as  
7  $+1.05 \text{ W m}^{-2}$  between 1870 and 1992 (Table 2). This is consistent with a radiative  
8 forcing of  $3.7 \text{ W m}^{-2}$  for a doubling of the  $\text{CO}_2$  concentration (Forster et al., 2007).

9

10 The RCM was also used to calculate the first order surface temperature reponse by  
11 allowing the tropospheric temperature and specific humidity readjust, but keeping the  
12 relative humidity and cloud cover unperturbed. Thus the water vapor and lapse rate  
13 feedback is incorporated, but no non-local feedbacks. In reponse to  $\text{CO}_2$  concentration  
14 change, shortwave radiation at the tropopause is adjusted slightly owing to the  
15 dependence of spectral cloud properties on temperature, but this effect was  $< 0.5\%$ .  
16 IPCC (Ramaswamy et al., 2001, Forster et al., 2007) notes that the inter-model  
17 differences are 10 % for detailed line-by-line radiation schemes and 20% for GCM  
18 radiation schemes (Collins et al., 2006, Forster and Taylor, 2006). The (change in)  
19 radiative forcing due to increasing  $\text{CO}_2$  concentrations ( $\text{RF}_{\text{CO}_2}$ ) is thus about five  
20 times larger than  $\text{RF}_{\text{lcc}}$  (table 2).

21

## 22 *b. EC-Earth calculations*

23 To perform the simulations, the EC-Earth global circulation model is used (Haarsma  
24 et al., 2009, see [eearth.knmi.nl](http://eearth.knmi.nl)). The model is a derivative of the Operational  
25 Seasonal Forecast System 3 of the Integrated Forecast System (IFS) of the European

1 Centre for Medium-Range Weather Forecast (ECMWF). The atmospheric model  
2 version is identical to IFS cycle 31r1, with spectral truncation T95 and 40 vertical  
3 levels. The ocean was represented by pre-scribed sea surface temperatures (SST) and  
4 sea-ice concentration (SIC), varying monthly and inter-annually after the Hadley  
5 Centre Ice and Sea Surface Temperature data set (Rayner et al., 2000, 2003). The  
6 global mean SST increased 0.33 °C between the pre-industrial and present-day era,  
7 whereas the global mean SIC decreased -0.6 % (from 6.2% to 5.6%) (Figure 1). The  
8 radiation code is identical to the formulation in the RCM used above. Doubling of  
9 CO<sub>2</sub> concentration leads to a radiative forcing of 3.7 W m<sup>-2</sup> (van Dorland, 1999),  
10 similar to other models as reported by Forster et al (2007 )

11

12 Four experiments were performed, 1) a ‘reference’ (r) experiment, with pre-industrial  
13 (1870) land cover and CO<sub>2</sub> concentration; 2) a ‘modified vegetation’ (v) experiment,  
14 where land cover was changed to the 1992 distribution (Figure 2); 3) a ‘modified CO<sub>2</sub>  
15 concentration’ (c) experiment, where CO<sub>2</sub> concentration was changed to the 1992  
16 level; and 4) a ‘modified vegetation and CO<sub>2</sub> concentration’ (vc) experiment, where  
17 both land cover and CO<sub>2</sub> concentration were changed to the present-day (1992)  
18 distribution/level. SST and SIC follow the CO<sub>2</sub> concentration.

19

20 Each experiment consisted of 5 ensemble runs of 10-year duration. In each  
21 consecutive run, the year of the SST and SIC was advanced 5 years, starting in 1870  
22 for the ‘r’ and ‘v’ runs and in 1972 for the ‘c’ and ‘vc’ runs. Hence each experiment  
23 covers in total 30 years with overlapping ensembles. The atmosphere was always  
24 initialised as on 1 January 1990. Potential spin-up errors were checked for by  
25 comparing soil moisture for the first year of a simulation with the corresponding

1 overlapping simulation, but the variability between years was generally larger than the  
2 difference between overlapping years. Therefore we use the complete time series in  
3 the analyses. The concentrations of CH<sub>4</sub>, N<sub>2</sub>O, CFC11, CFC12 were changed  
4 proportional to the CO<sub>2</sub> concentrations. SST and SIC data were obtained from Hadley  
5 Centre HadISST data set (Rayner et al., 2000, 2003).

6  
7 Time series of the fractional cover of pasture and crops were obtained from Klein  
8 Goldewijk (2001) and Ramankutty and Foley (1999), respectively (figure 2), and  
9 implemented in the land surface scheme of EC-Earth. 20 different plant functional  
10 types are discerned, that are distributed into high and low vegetation types (Van den  
11 Hurk et al, 2000). Each grid cell is attributed only one dominant high vegetation type  
12 and one low vegetation type, with assigned fractions for each. The vegetation type  
13 determines vegetation characteristics such as leaf area index, surface roughness,  
14 minimum stomatal resistance and root depth. Originally, EC-Earth uses a satellite  
15 derived background albedo map, but for the purpose of this study, we used albedo  
16 maps derived by correlation of background albedo with fraction of each vegetation  
17 type, on a monthly and zonal mean basis. Albedo fields were produced that  
18 correspond with the vegetation maps for 1870 and 1992. The model data are presented  
19 as temporal means on a 1° by 1° grid.

20

21 The change in net radiation ( $\Delta R_n$ ) at the top of the atmosphere is the net effect of the  
22 radiative forcing (RF) and the feedbacks of the climate system. The difference  
23 between the change in net radiation and the radiative forcing is thus a measure of the  
24 strength of feedbacks. According to the IPCC definition (Forster et al., 2007) radiative  
25 forcing is defined at the top of the atmosphere or at the tropopause, and not at the

1 surface, because below the tropopause significant parts of energy exchange are non-  
2 radiative. The change in net radiation in EC-Earth at the top of the atmosphere was  
3 assumed to represent the radiative forcing at the tropopause for two reasons. First,  
4 after stratospheric adjustment, the radiative forcing due to CO<sub>2</sub> is identical at the two  
5 levels (Harvey, 2000). Second, since the stratosphere is nearly transparent for  
6 shortwave radiation, the radiative forcing due to land cover change is also similar at  
7 the tropopause and TOA.

8

9 The experimental set-up does not allow a response of SSTs and SIC to the applied  
10 forcings. The implications of this are discussed below.

11

### 12 **3. Results**

13 The EC-Earth model results represent the combined effect of radiative forcing and  
14 feedbacks, and hence we will use the term ‘change in net radiation’ when referring to  
15 model results. A schematic comparison between the RCM estimate of radiative  
16 forcing and the change in net radiation in EC-Earth is presented in table 3. The RCM  
17 estimate of the radiative forcing due to land cover change (v),  $RF_{lcc} = -0.19 \text{ W m}^{-2}$  is  
18 very similar to EC-Earth’s change in net radiation ( $-0.20 \text{ W m}^{-2}$ ), which suggests the  
19 existence of only small feedbacks in EC-Earth. For the impact of increasing CO<sub>2</sub>  
20 concentration (c), EC-Earth gives a larger change in net radiation than the RCM  
21 radiative forcing (1.51 vs.  $1.05 \text{ W m}^{-2}$ ), suggesting that positive feedbacks are active.  
22 EC-Earth suggests that the impacts of land cover change and increasing CO<sub>2</sub>  
23 concentration appear to be linearly additive, as the sum of the simulations with only  
24 land cover change ( $-0.20 \text{ W m}^{-2}$ ) and CO<sub>2</sub> concentration change ( $+1.51 \text{ W m}^{-2}$ )  
25 closely resembles the simulation with the joint changes ( $+1.33 \text{ W m}^{-2}$ ).

1

2 *a. Global climate sensitivity and feedbacks*

3 In this section we compare the sensitivity of global mean climate to changes in land  
4 cover and CO<sub>2</sub> concentration. The climate sensitivity parameter  $\lambda$  is determined as:

5 
$$\lambda = \frac{\Delta T_{2m}}{\Delta RF}$$

6 with  $\Delta T_{2m}$  is the change in air temperature at 2 m height (labelled as “surface  
7 temperature” below) and  $\Delta RF$  the change in radiative forcing (IPCC, Forster et al.,  
8 2007). The radiative forcing and climate sensitivity are useful metrics here, because  
9 they allow a direct comparison between the impact of land cover and CO<sub>2</sub> change on  
10 the climate system.

11

12 1) CLIMATE SENSITIVITY

13 The (change in) radiative forcing due to land cover change between 1870 and 1992,  
14 deduced from the RCM calculations, is -0.19 W m<sup>-2</sup>. The surface temperature change  
15 calculated by EC-Earth of -0.04 °C is considerably less than the -0.12 °C from the  
16 RCM (Table 2). The (change in) radiative forcing due to the increase in CO<sub>2</sub> from 288  
17 ppm in 1870 to 356 ppm in 1992 is 1.05 W m<sup>-2</sup> and is associated with a surface  
18 temperature change of +0.51 °C, slightly less than the value of 0.61 °C from the  
19 RCM. The resulting climate sensitivities (calculated using EC-Earth temperature  
20 change and RCM radiative forcings) are shown in Fig. 3. Our experiments were  
21 performed with prescribed SST and SIC, which were varied with CO<sub>2</sub> concentration,  
22 but not with land cover. This implies the underlying assumption that land cover  
23 change did not cause a change in SST and SIC. We verified this assumption by  
24 calculating the climate sensitivity parameter for the entire globe (land and ocean) and  
25 for land alone (Fig. 3). The climate sensitivity to land cover change can be obtained at

1 historic (v-r) and present times (vc-c). Similarly, the climate sensitivity to CO<sub>2</sub>  
2 concentration can be obtained at historic (c-r) and present land cover (vc-v). The two  
3 realizations of climate sensitivity to land cover change appear to be identical,  $\lambda_{(v-r)} =$   
4  $\lambda_{(vc-c)} = 0.22 \text{ } ^\circ\text{C} / \text{W m}^{-2}$  (Fig. 3). In the same way, the two realizations of climate  
5 sensitivity to CO<sub>2</sub> concentration change are identical,  $\lambda_{(c-r)} = \lambda_{(vc-v)} = 0.49 \text{ } ^\circ\text{C} / \text{W m}^{-2}$ .  
6 The robustness of the climate sensitivity parameters suggests that the temperature  
7 response to land cover change is not dominated by the prescribed SIC and SST, but  
8 rather by the forcing itself.

9

10 The climate sensitivity to land cover change,  $\lambda_{lcc}$ , is the same for the global scale (0.22  
11  $^\circ\text{C} / \text{W m}^{-2}$ ) and for the land alone (where the  $\text{RF}_{lcc}$  over land is calculated as the  
12 global  $\text{RF}_{lcc}$  divided by the land fraction,  $-0.19 / 0.34 = -0.56 \text{ W m}^{-2}$ ). Considering that  
13 the radiative forcing only occurs over land, the similarity suggests that the  
14 temperature change occurs primarily over land as well. This may be partly explained  
15 by the local character of land cover change and the absence of persistent  
16 teleconnections (Pitman et al., 2009), but also by the prescribed SST and SIC. This is  
17 further discussed in section 4. In contrast, the climate sensitivity to CO<sub>2</sub> concentration  
18 change,  $\lambda_{co2}$ , is smaller globally ( $0.49 \text{ } ^\circ\text{C}/\text{W m}^{-2}$ ) than over land alone ( $0.63 \text{ } ^\circ\text{C}/\text{W m}^{-2}$ ).  
19 The  $\lambda_{co2} = 0.42 \text{ } ^\circ\text{C}/\text{W m}^{-2}$  over ocean (not shown) is to a large extent determined by  
20 the prescribed change in SST and SIC between 1870 and 1992. The fact that  $\lambda_{co2}$  is  
21 different over land and ocean indicates that the response over land is not entirely  
22 dominated by the fixed SST. It may also indicate that feedback mechanisms are  
23 different over land and over ocean.

24

1 The climate sensitivity of simultaneous land cover and CO<sub>2</sub> concentration change  
2 does not appear to be a useful metric, because both the radiative forcings and  
3 temperature responses are of opposite sign and compensating, leading to ill-posed  
4 ratios.

5

## 6 2) QUANTIFICATION OF FEEDBACKS

7 Above, it was shown that the climate sensitivity to land cover change,  $\lambda_{lcc}$ , is smaller  
8 than the climate sensitivity to CO<sub>2</sub> concentration change  $\lambda_{co2}$  (Fig. 3). This implies  
9 that one or more feedback mechanisms are active, and that the feedbacks to land cover  
10 change are different than to CO<sub>2</sub> concentration change. We quantify the net feedback  
11 as the difference between primary radiative forcing and the resulting change in TOA  
12 net radiation. We use a decomposition in short- and long wave components, and  
13 analyse the changes in surface temperature and total cloud fraction.

14

15 Table 4 displays the results of the feedback analysis. Both land cover and CO<sub>2</sub> change  
16 are associated with feedbacks. We define a factor  $r = dR_n / RF$  as the relative impact  
17 of feedbacks, with  $dR_n$ , the change in net radiation as in table 4.  $r = 1$  indicates zero  
18 impact,  $r < 1$  indicates negative (damping) feedbacks and  $r > 1$  indicates positive  
19 (amplifying feedbacks). In our experiments,  $r_{lcc} = 0.97$  and  $r_{co2} = +1.44$ . Apparently,  
20 CO<sub>2</sub> concentration change is associated with positive feedbacks, whereas land cover  
21 change is not associated with net feedbacks.

22

23 Land cover change (mainly deforestation) causes a small increase in global mean total  
24 cloud cover of +0.02 % (Table 4). Figure 4 shows the spatial structure of the cloud  
25 cover change, revealing decreasing high clouds and increasing low cloud cover at NH

1 mid latitudes, and decreasing both high and low cloud cover in tropical deforested  
2 regions (hotspots in South America, Africa and Indonesia) presumably related to deep  
3 convection. This regionally varying response is further discussed below. In the tropics  
4 the albedo induced net radiation reduction leads to decreases in the sensible heat flux,  
5 locally up to  $-15 \text{ W m}^{-2}$ , and much smaller decreases in the latent heat flux (see  
6 below). The global averaged effect is that the net shortwave radiation does not  
7 significantly change, but the net long wave radiation increases with  $+0.07 \text{ W m}^{-2}$ ,  
8 indicating a reduction in long wave radiation emission to space. This is a damping  
9 feedback to the negative radiative forcing due to land cover change.

10

11  $\text{CO}_2$  concentration change is associated with a decrease in total cloud fraction by -  
12 0.50 % (Table 4), which is mostly confined to the subtropical oceans, whereas total  
13 cloud cover increases in a few narrow zones around the equatorial oceans (Fig. 4,  
14 right). These changes are mainly due to changes in high clouds and may be attributed  
15 to a shift in the Inter Tropical Convergence Zone (ITCZ), as a result of acceleration of  
16 the hydrological cycle in a warmer climate (Held and Soden, 2006). Decreasing cloud  
17 cover is observed in the arctic and southern oceans, which is related to changes in SIC  
18 and SST (Fig. 1). Changes in these areas are primarily due to decreases in low cloud  
19 cover. Over land the decreases are generally much weaker than over the oceans, but  
20 are considerable in the boreal areas of Canada and Siberia. In areas where cloud cover  
21 decreases, net shortwave radiation increases (+ve feedback to  $\text{RF}_{\text{CO}_2}$ ) and net long  
22 wave radiation decreases (-ve feedback). The +ve shortwave feedback is stronger than  
23 the -ve long wave feedback, resulting in a strong overall amplification of the forcing.

24

25 *b. Regional variation in feedbacks*

1) THE REGIONAL EFFECT OF LAND COVER CHANGES ALONE (V)

The primary impact of land cover change is through albedo. Fig. 5 (top left) shows the net shortwave radiation changes as a function of albedo at the TOA. Areas with negative albedo changes are few, and mainly associated with reforestation. The direct shortwave radiative forcing is linearly proportional to the surface albedo and represented by the straight lines, which are steeper in the tropics than in the mid-latitudes, because of the higher solar insolation. The change in net shortwave radiation, including feedbacks is represented by the lines with error bars. In the NH mid-latitudes, the net effect is very similar to the direct radiative forcing for positive albedo changes, suggesting the absence of feedbacks. In the tropics, the change in net shortwave radiation is much smaller than the direct response, suggesting the presence of damping feedbacks, associated with a decrease in cloud cover.

Concerning the response of net long wave radiation to land cover change, again a distinct difference exists between tropical zones and NH mid-latitude zones (Fig. 5, top right). In NH mid-latitude zones, the net long wave radiation increases, and thus partly compensates the decrease in net shortwave radiation. In tropical zones, the net long wave radiation decreases, and thus amplifies the decrease in net shortwave radiation associated with albedo increases. The decrease in net long wave radiation in tropical deforested regions (implying an increase in outgoing long wave radiation at the TOA) is consistent with the decrease in high and low cloud cover after deforestation (Fig. 4). In contrast, the increase in net long wave radiation in NH mid-latitudinal deforested regions is associated with increased cloud cover (Fig. 5 bottom right). However, as it is mainly an increase in low cloud cover that is seen in this region (Fig. 4), increased long wave emission and reduced net surface long wave

1 radiation are indeed expected. The changes in radiation balance and cloud cover cause  
2 changes in the surface temperature (Fig. 6) and the surface net radiation partitioning  
3 (Fig. 7). Although cause and effect are intimately related, the net effect is a strong  
4 surface temperature decrease in the NH mid latitudes and nearly no surface  
5 temperature change in the tropics. Sensible heat flux decreases similarly in both  
6 climate zones, and latent heat flux decreases only in the tropics, but less than the  
7 sensible heat flux.

8

9 As a result, in both climate zones the change in net all wave radiation is smaller than  
10 the radiative forcing, particularly in the tropics (Fig. 5 bottom left). Because land  
11 cover change occurred for the most part in the NH mid-latitudes, where the change in  
12 net radiation is close to the radiative forcing, on a global scale the net effect of  
13 feedbacks are only slightly damping ( $r = 0.97$ ). In the tropics the damping is primarily  
14 a result of shortwave radiation responses associated with cloud cover, whereas at the  
15 NH mid latitudes a long wave damping is related to small cloud cover increases and  
16 surface cooling. In the tropics this surface cooling is offset by a reduced latent heat  
17 release, which is virtually absent in the NH mid latitudes. The response applies to  
18 both the surface level and the top of the atmosphere (not shown).

19

20 2) THE REGIONAL EFFECT OF INCREASING CO<sub>2</sub> CONCENTRATION ALONE

21 (C)

22 The increase in net long wave radiation at the surface is spatially rather uniformly  
23 distributed (Fig. 8, top left). Overall, the surface net long wave radiation has increased  
24 due to the increased CO<sub>2</sub> concentration. The peaks at high latitudes are caused by the  
25 changes in the surface temperature. In contrast, there is a strong zonal response in the

1 net shortwave radiation (Fig. 8, top right). The peaks poleward of  $45^\circ$  are associated  
2 with changes in snow and sea ice cover and associated albedo. For instance, on the  
3 NH the change in the Okhotsk Sea between Sakhalin and Kamtsjatka ( $50^\circ\text{N}$ ) is  
4 notable. Also a sharp decrease in net shortwave radiation occurs near the equator in  
5 the Indian and East Pacific Ocean, which is accompanied by increases just North and  
6 South of this area ( $\sim 10\text{-}30^\circ$ ). Over land a similar but weaker pattern is observed. The  
7 patterns show increased cloud cover near the equator and decreased cloud cover in  
8 the subtropics (Fig. 4), and may indicate an intensification or widening of the ITCZ.  
9 The global average changes in net long wave and shortwave radiation at the surface  
10 are  $+1.4 \text{ W m}^{-2}$  and  $+0.03 \text{ W m}^{-2}$ , respectively. The latter is the balance of increased  
11 net shortwave radiation poleward of  $45^\circ$  due to snow and sea ice (averaging  $+0.17 \text{ W}$   
12  $\text{m}^{-2}$ ) and the change in net shortwave radiation equator ward of  $\pm 45^\circ$  due to the change  
13 in cloud cover (averaging  $-0.03 \text{ W m}^{-2}$ ). The larger surface area in the tropics causes  
14 the two terms to nearly cancel.

15

16 At the top of the atmosphere, the change in net shortwave radiation is similar to the  
17 surface response (Fig. 8, bottom right). However, the net long wave radiation change  
18 pattern is very different (Fig. 8, bottom left). In fact, in the tropics the change in net  
19 long wave radiation at the top of the atmosphere resembles the opposite of the change  
20 in net shortwave radiation. This may be explained by changes in cloud cover: at the  
21 equator, increased cloudiness causes a decrease in net shortwave radiation and an  
22 increase in net long wave radiation (less long wave cooling) due to surface masking  
23 effect of clouds. In the subtropics, the opposite occurs.

24

1 3) THE REGIONAL EFFECT OF SIMULTANEOUS LAND COVER CHANGE  
2 AND INCREASED CO<sub>2</sub> CONCENTRATION

3 In table 3 the effects of land cover change and increasing CO<sub>2</sub> concentration on net  
4 radiation were shown to be linearly additive on the global scale. In this section, we  
5 look at spatial variability of a number of variables. We compare the sum of the  
6 response to the individual forcings (v-r) + (c-r) to the combined forcing (vc-r) by  
7 means of linear regression. Strong departures from a linear relation between (v-r)+(c-  
8 r) and (vc-r) point at significant non-linear feedbacks between these forcings. Table 5  
9 presents the statistics Root Mean Square Error (RMSE), correlation coefficient ( $r^2$ )  
10 and slope of the change in the respective variable in (v-r) + (c-r) as a function of the  
11 change in (vc-r). The RMSE is small relative to the total change (not shown),  $r^2$  is  
12 typically larger than 0.85 and slopes are close to 1 for most variables, except long  
13 wave radiation, cloud cover, precipitation and soil moisture. This applies both  
14 globally (upper part of table 5) and to areas with extensive land cover change (lower  
15 part). Hence, in general the sum of changes in the experiments (v-r) and (c-r)  
16 compares well with the joint land cover and CO<sub>2</sub> concentration change experiment.

17

18 Long wave radiation, cloud cover, precipitation and soil moisture are variables related  
19 to water, where non-linearities in feedbacks and ‘memory’ may play a larger role than  
20 for radiative and heat fluxes. It appears that Australia and the Middle-East are regions  
21 where the correlation is lowest for those variables (not shown), which is remarkable  
22 because these regions are not subject to large-scale land cover change. Consequently,  
23 this must be the result of non local-feedbacks that occur differently in the ‘vc’  
24 experiment than in the sum of ‘v’ and ‘c’ experiments. Nevertheless, there are no

1 indications that non-linear feedbacks between land cover and CO<sub>2</sub> change occur on a  
2 large scale.

3

#### 4 **4. Discussion**

5 Our experiments were performed in the context of the LUCID (Land Use Change,  
6 IDentification of robust factors) inter-comparison study, where seven climate models  
7 were used to perform experiments with a similar setup (Pitman et al., 2009). Amongst  
8 these models, EC-Earth occupied an average position with regard to the magnitude  
9 and direction of changes in regions subject to land cover change: the change in latent  
10 heat flux (LE) was in the same range as three other models, with LE decreasing with  
11 10-20 W m<sup>-2</sup>; the temperature changes were large (maximum -2 °C) but in the same  
12 order as three other models, and confined to the NH mid latitudes. No pronounced  
13 pattern in precipitation changes was simulated by EC-Earth, similar to all other  
14 models. EC-Earth did not display significant teleconnections, as all other models  
15 (Pitman et al., 2009).

16

17 The experimental design of this first LUCID phase used prescribed SST and SIC. As a  
18 result, there is no interactive temperature and humidity flux between ocean and  
19 atmosphere, and the oceans form a theoretically unlimited source or sink of heat.  
20 However, since the SST and SIC are prescribed with seasonal and inter-annual  
21 variability based on observations (Rayner et al., 2000, 2003) the SST and SIC are  
22 realistic. The only true limitation of the current set-up is a lack of feedbacks between  
23 ocean and climate, which however, generally act on time scales longer than our  
24 experiments. The larger climate sensitivity over land (0.63 °C/ W m<sup>-2</sup>) than the global  
25 average (0.49 °C/ W m<sup>-2</sup>) is observed in other coupled models as well, and is

1 attributed to the shorter temperature response time of land than of ocean (IPCC,  
2 Randall et al., 2007; Hegerl et al., 2007).

3

4 Climate sensitivity is defined as the ratio of global average near surface temperature  
5 change and radiative forcing. For moderate radiative forcings that do not push the  
6 climate system in another state (Boer et al., 2005), the climate sensitivity for a  
7 particular type of forcing has been found to be constant within  $\pm 20\%$  within models,  
8 being largely independent on its latitudinal or vertical structure (Hansen et al., 1997,  
9 Boer and Yu, 2003). This proportionality of temperature change and radiative forcing  
10 was confirmed for forcing types such as doubling of CO<sub>2</sub>, variations in solar  
11 luminosity, and even regionally concentrated non-absorbing aerosols (Cox et al.,  
12 1995). No solid physical principle behind the proportionality exists, but it does  
13 indicate that feedback mechanisms have a pronounced physical cause. In fact, the  
14 constant of proportionality, i.e. the climate sensitivity, is a measure of the effect of  
15 feedbacks. The climate sensitivity we refer to represents the transient climate  
16 sensitivity, i.e. the transient climate response (TCR) scaled with radiative forcing. The  
17 transient climate sensitivity differs from the equilibrium climate sensitivity, in that it  
18 is usually smaller and more relevant to near future climate. TCR values for a doubling  
19 of the CO<sub>2</sub> concentration reported in literature are in the range of 1.6 °C (Knutti and  
20 Tomassini, 2008), 1.5-2.8 °C (median 2.1 °C, Stott et al., 2006), 1.2-2.6 °C (median  
21 of 1.6 °C, IPCC, Randall et al., 2007) and 2.5-3.6 °C (Tung et al., 2008). Scaling with  
22 radiative forcing results in climate sensitivities of 0.32 to 0.97 °C/W m<sup>-2</sup>. With EC-  
23 Earth we found a climate sensitivity to CO<sub>2</sub> concentration change of  $\lambda_{\text{CO}_2} = 0.49^\circ\text{C}/\text{W}$   
24 m<sup>-2</sup>, which is close to the median of IPCC AR4 (0.43 °C/W m<sup>-2</sup>).

25

1 Our climate sensitivity to land cover change  $\lambda_{lcc} = 0.22 \text{ }^\circ\text{C/W m}^{-2}$  may be compared  
2 with values given in other studies:  $0.60 \text{ }^\circ\text{C/W m}^{-2}$  in the RCM of Van Dorland  
3 (1999),  $0.70 \text{ }^\circ\text{C/W m}^{-2}$  (transient climate sensitivity, Hansen et al., 1998),  $0.65 \text{ }^\circ\text{C / W}$   
4  $\text{m}^{-2}$  (1750-2000, transient, intermediate complexity earth system model with coupled  
5 ocean model, Matthews et al., 2004),  $0.65\text{-}1.25 \text{ }^\circ\text{C / W m}^{-2}$  (6 intermediate  
6 complexity models, transient climate sensitivity, Brovkin et al., 2006),  $0.52$  and  $0.38$   
7  $^\circ\text{C/W m}^{-2}$  (1860 to 1992 and 1992 to 2100, equilibrium climate sensitivity, fully  
8 coupled ocean and ice model, Davin et al., 2003), and  $0.50 \text{ }^\circ\text{C / W m}^{-2}$  (equilibrium,  
9 conversion of entire land surface from grassland to trees, Gibbard et al., 2005). The  
10 cited studies cover a range of complexity and approaches, and yield climate  
11 sensitivities in the range between  $0.38$  and  $1.25 \text{ }^\circ\text{C / W m}^{-2}$ , with values close to  $0.6$   
12  $^\circ\text{C / W m}^{-2}$  being often reported. This is somewhat larger than the climate sensitivity  
13 to  $\text{CO}_2$  concentration change. The small climate sensitivity to land cover change in  
14 EC-Earth ( $0.22 \text{ }^\circ\text{C / W m}^{-2}$ ) suggests that damping feedbacks are apparently stronger  
15 than usual. The sensitivity is possibly damped by the prescribed SST and SIC. This is  
16 illustrated by the changes in net surface sensible and latent heat fluxes in response to  
17 land cover change:  $\Delta H = +0.02 \text{ W m}^{-2}$  and  $\Delta LE = +0.07 \text{ W m}^{-2}$ . This indicates that  
18 cooling by  $\text{RF}_{lcc} = -0.19 \text{ W m}^{-2}$  is partly compensated by  $+0.09 \text{ W m}^{-2}$  heat release by  
19 the oceans. If this would be considered as a (pseudo)radiative forcing, the climate  
20 sensitivity would be  $\lambda_{lcc} = -0.04 / (-0.19 + 0.09) = 0.40 \text{ }^\circ\text{C / W m}^{-2}$ , which compares  
21 better with the studies cited above. The extra oceanic heat release is a response of to  
22 the cooling of the atmosphere, which demonstrates that LCC induced cooling affects  
23 energy balance terms elsewhere in the system. The fact that the climate sensitivity is  
24 the same over land alone as over land and ocean (Fig. 3,  $0.22 \text{ }^\circ\text{C / W m}^{-2}$ ) combined  
25 with the fact that LCC occurs only over land indeed implies that LCC induced cooling

1 is entirely compensated by oceanic heat release. Further causes for the relatively small  
2 climate sensitivity may be related to the absence of a surface temperature response in  
3 tropical regions of deforestation, even though this is also observed in some other  
4 models in the LUCID inter-comparison (Pitman et al., 2009). Particular choices in the  
5 set-up of the land model (no seasonal changes in roughness, no seasonal cycle in leaf  
6 area index, uniform soil types across the globe (van den Hurk et al, 2000), may be  
7 related to this response. The oceanic heat fluxes to the atmosphere may not be realistic  
8 in this atmospheric model intercomparison set-up, because the ocean cannot respond  
9 to the fluxes. However, further studies with coupled ocean models are foreseen.

10

11 The presence of clouds is a very prominent modulator of the radiation balance on  
12 earth. Clouds change the earth albedo from about 0.10 to 0.30, an impact much larger  
13 than the radiative forcings of land cover and CO<sub>2</sub> concentration change. For this  
14 reason, we explicitly showed the change in cloud fraction due to land cover and CO<sub>2</sub>  
15 change (Fig. 4), indicating the cloud feedback. However, there are more feedback  
16 mechanisms. We also showed the impact of snow and ice albedo on the radiative  
17 balance. A potentially important feedback mechanism to deforestation, that is  
18 probably not resolved in coarse models, is the modification of the sea breeze strength,  
19 that possibly enhances deep convection above small islands and affects the Hadley  
20 circulation (van der Molen et al., 2006). However, quantification of the impact of  
21 individual feedback mechanisms is outside the scope of this paper, where we intend to  
22 compare the relative effect of land cover and CO<sub>2</sub> concentration change on climate.

23

## 24 **5. Conclusions**

1 Using a Radiative-Convective Model (RCM) we calculated the radiative forcings of  
2 historic (1870 – 1992) land cover change and CO<sub>2</sub> concentration to be of opposite  
3 sign and different by about a factor five namely -0.19 W m<sup>-2</sup> and +1.05 W m<sup>-2</sup>,  
4 respectively. We used EC-Earth to study the sensitivity of climate to these two types  
5 of radiative forcings, and found transient climate sensitivities of 0.22 °C / W m<sup>-2</sup> and  
6 0.49 °C / W m<sup>-2</sup> due to changes in land cover and CO<sub>2</sub>, respectively. The model  
7 results indicate that land cover change is associated with damping feedbacks of -3 %,  
8 whereas CO<sub>2</sub> concentration change is associated with amplifying feedbacks of +44 %.  
9 This implies that the negative change in radiative forcing due to land cover change  
10 has a much smaller cooling effect than the warming effect of a positive change in  
11 radiative forcing due to CO<sub>2</sub> change. The response to land cover change is confined to  
12 the region of the land cover change, and is zonally variable: in the mid-latitudes it has  
13 a cooling effect, and in the tropics a negligible effect on surface temperature due to  
14 compensating feedbacks involving the surface energy balance. The climate sensitivity  
15 of EC-Earth to land cover change is smaller than reported in literature. This may be  
16 partly explained by the prescribed SST, which compensated LCC induced cooling by  
17 heat release from the ocean. The response to CO<sub>2</sub> concentration change has a global  
18 character, with a clear polar amplification due to snow and ice melt, and associated  
19 changes in cloud cover. In tropical regions, changes in cloud cover may be attributed  
20 to changes in the ITCZ and the hydrological cycle. The impacts of land cover and  
21 CO<sub>2</sub> change appear reasonably linearly additive, with a possible exception for  
22 variables related to hydrology, as a result of time lags. The correct representation of  
23 the impact of land cover and CO<sub>2</sub> change in climate models is important for  
24 understanding, attributing and projecting ongoing climate change.  
25

1 *Acknowledgements.* Rob van Dorland assisted with the calculations of the RCM,  
2 which is greatly appreciated. We thank Xueli Wang for her help setting up the  
3 experiments. The organizers of the LUCID campaign are acknowledged, in particular  
4 Nathalie de Noblet, Andy Pitman and Faye Cruz. The Dutch Research Organization  
5 (NWO) sponsored parts of this study.

6

## 7 **References**

- 8 Betts, R.A., 2001: Biogeophysical impacts of land use on present-day climate: near-  
9 surface temperature change and radiative forcing. *Atmos. Sci. Lett.*, **2**, (1-4),  
10 doi:1006/asle.2001.0023
- 11
- 12 Betts, R.A., P.D. Falloon, K. Klein Goldewijk, N. Ramankutty, 2007: Biogeophysical  
13 effects of land use on climate: Model simulations of radiative forcing and large-scale  
14 temperature change. *Agric. For. Meteorol.*, **142**, 216-233.
- 15
- 16 Boer, G.J. and B. Yu, 2003: Climate sensitivity and response. *Clim. Dyn.*, **20**, 415–  
17 429, DOI 10.1007/s00382-002-0283-3
- 18
- 19 Boer, G.J., K. Hamilton and W. Zhu, 2005: Climate sensitivity and climate change  
20 under strong forcing. *Clim. Dyn.*, **24**, 685–700. DOI 10.1007/s00382-004-0500-3
- 21
- 22 Bony, S., R. Colman, V.M. Kattsov, R.P. Allan, C.S. Bretherton, J.-L. Dufresen, A.  
23 Hall, S. Hallegatte, M.M. Holland, W. Ingram, D.A. Randall, B.J. Soden, G.  
24 Tselioudis and M.J. Webb, 2006: How well do we understand and evaluate climate  
25 change feedback processes? *J. Clim.*, **19**, 3445-3482.

1

2 Bounoua, L., R. Defries, G.J. Collatz, P. Sellers and H. Kahn, 2002: Effects of land  
3 cover conversion on surface climate. *Clim. Change*, **52**, 29-64.

4

5 Brovkin, V., S. Sitch, W. von Bloh, M. Claussen, E. Bauer and W. Cramer, 2004:  
6 Role of land cover changes for atmospheric CO<sub>2</sub> increase and climate change during  
7 the last 150 years. *Glob. Ch. Biol.*, **10**, 1253-1266.

8

9 Brovkin, V., M. Claussen, E. Driesschaert, T. Fichefet, D. Kicklighter, M. F. Loutre  
10 H. D. Matthews, N. Ramankutty, M. Schaeffer, A. Sokolov, 2006: Biogeophysical  
11 effects of historical land cover changes simulated by six Earth system models of  
12 intermediate complexity. *Clim. Dyn.*, **26**, 587-600, DOI 10.1007/s00382-005-0092-6

13

14 W. D. Collins, V. Ramaswamy, M. D. Schwarzkopf, Y. Sun, R. W. Portmann, Q. Fu,  
15 S. E. B. Casanova, J.-L. Dufresne, D. W. Fillmore, P. M. D. Forster, V. Y. Galin, L.  
16 K. Gohar, W. J. Ingram, D. P. Kratz, M.-P. Lefebvre, J. Li, P. Marquet, V. Oinas, Y.  
17 Tsushima, T. Uchiyama, W. Y. Zhong, 2006: Radiative forcing by well-mixed  
18 greenhouse gases: Estimates from climate models in the IPCC AR4. *J. Geophys.*  
19 *Res.*, **111**, D14317, doi: 10.1029/2005JD006713.

20

21 Cox, S., W.-C. Wang, and S. Schwartz, 1995: Climate Response to Radiative  
22 Forcings by Sulfate Aerosols and Greenhouse Gases. *Geophys. Res. Lett.*, **22**,(18),  
23 2509-2512.

24

1 Cox, P.M., R.A. Betts, C.D. Jones, S.A. Spall, and I.J. Totterdell, 2000: Acceleration  
2 of global warming due to carbon cycle feedbacks in a coupled climate model. *Nature*,  
3 **408**, 6809, 184-187.

4

5 Davin, E. L., N. de Noblet-Ducoudre', and P. Friedlingstein, 2007: Impact of land  
6 cover change on surface climate: Relevance of the radiative forcing concept. *Geophys.*  
7 *Res. Lett.*, **34**, L13702, doi:10.1029/2007GL029678

8

9 Dessler, A.E. and S.E. Sherwood, 2009: A matter of humidity; *Science*, **232**, 1020-  
10 1021, doi: 10.1126/science.1171264

11

12 Feddema, J.J., K.W. Oleson, G.B. Bonan, L.O. Mearns, L.E. Buja, G.A. Meehl,  
13 W.M. Washington, 2005: The importance of land-cover change in simulating future  
14 climates. *Science*, **310**, 1674-1678.

15

16 Forster, P.M.F and K.E. Taylor, 2006: Climate forcings and climate sensitivities  
17 diagnosed from coupled climate model integrations. *J. Clim.*, **19**, 6181-6194.

18

19 Forster, P., V. Ramaswamy, P. Artaxo, T. Berntsen, R. Betts, D.W. Fahey, J.  
20 Haywood, J. Lean, D.C. Lowe, G. Myhre, J. Nganga, R. Prinn, G. Raga, M. Schulz  
21 and R. van Dorland, 2007: Changes in Atmospheric constituents and in radiative  
22 forcing. *Climate change 2007: The physical basis, contribution of Working group I to*  
23 *the fourth assessment report of the Intergovernmental Panel of Climate Change*, S.

24 Solomon, D. Qin, M. Manning, Z. Chen, M. Marquis, K.B. Averyt, M. Tignor and

1 H.L. Miller, Eds., Cambridge University Press, Cambridge, United Kindom and New  
2 York, NY, USA, 129-234.

3

4 Friedlingstein, P., J.-L. Dufresne, P.M. Cox and P. Rayner, 2003: How positive is the  
5 feedback between climate change and the carbon cycle. *Tellus*, **55B**, 692-700.

6

7 Gibbard, S., K. Caldeira, G. Bala, T. J. Phillips, and M. Wickett, 2005: Climate  
8 effects of global land cover change, *Geophys. Res. Lett.*, **32**, L23705,  
9 doi:10.1029/2005GL024550.

10

11 Haarsma, R.J., F.M. Selten, B.J.J.M. van den Hurk, W. Hazeleger en X. Wang, 2009:  
12 Drier Mediterranean Soils due to Greenhouse Warming bring easterly Winds over  
13 Summertime Central Europe. *Geophys. Res. Lett.*, **36**, L04705,  
14 doi:10.1029/2008GL036617.

15

16 Hansen, J., M. Sato and R. Ruedy, 1997: Radiative forcing and climate response. *J.*  
17 *Geophys. Res.*, **102**, (D6), 6831-6864.

18

19 Hansen, J.E., M. Sato, A. Lacis, R. Ruedy, I. Tegen, and E. Matthews, 1998: Climate  
20 forcings in the Industrial era. *Proc. Natl. Acad. Sci. USA*, **95**, 12753–12758.

21

22 Harvey, L.D.D., 2000: Global Warming, the hard science. Prentice-Hall, Harlow, UK.

23

24 Klein Goldewijk, K., 2001: Estimating global land-use change within the past 300  
25 years: the HYDE database. *Glob. Biogeochem. Cycl.*, **15**, 417-433.

1

2 Hegerl, G.C., F. W. Zwiers, P. Braconnot, N.P. Gillett, Y. Luo, J.A. Marengo Orsini,  
3 N. Nicholls, J.E. Penner and P.A. Stott, 2007: Understanding and Attributing Climate  
4 Change. *Climate Change 2007: The Physical Science Basis. Contribution of Working*  
5 *Group I to the Fourth Assessment Report of the Intergovernmental Panel on Climate*  
6 *Change.*, S. Solomon, D. Qin, M. Manning, Z. Chen, M. Marquis, K.B. Averyt, M.  
7 Tignor and H.L. Miller, Eds. Cambridge University Press, Cambridge, United  
8 Kingdom and New York, NY, USA.

9

10 Held, I.M. and B.J. Soden, 2006: Robust responses of the hydrological cycle to Global  
11 warming; *J.Clim.*, **19**, 5686-5699.

12

13 Knutti, R., and L. Tomassini, 2008: Constraints on the transient climate response from  
14 observed global temperature and ocean heat uptake, *Geophys. Res. Lett.*, **35**, L09701,  
15 doi:10.1029/2007GL032904.

16

17 Manabe, S. and R.F. Strickler, 1964: Thermal equilibrium of the atmosphere with a  
18 convective adjustment. *J. Atm.. Sci.*, **21**, 361-385.

19

20 Manabe, S., and R. T. Wetherald, 1967: Thermal equilibrium of the atmosphere with a  
21 given distribution of relative humidity. *J. Atm.. Sci.*, **24**, 241-259.

22

23 Matthews, H.D., A.J. Weaver, K.J. Meissner, N.P. Gillett and M. Eby, 2001: Natural  
24 and anthropogenic climate change: incorporating historical land cover change,  
25 vegetation dynamics and the global carbon cycle. *Clim. Dyn.*, **22**, 461-479.

1

2 Pitman, A.J. and M. Zhao, 2000: The relative impact of observed change in land cover  
3 and carbon dioxide as simulated by a climate model. *Geophys. Res. Lett.*, **27**, (9),  
4 1267-1270.

5

6 Pitman, A.J., N. de Noblet-Ducoudré, F.T. Cruz, E.L. Davin, G.B. Bonan, V. Brovkin,  
7 M. Claussen, C. Delire, L. Ganzeveld, V. Gayler, B.J.J.M. van den Hurk, P.J.  
8 Lawrence, M.K. van der Molen, C. Müller, C.H. Reick, S.I. Seneviratne, B.J.  
9 Strengers and A. Voldoire, 2009: Land-Use and climate via the LUCID

10 intercomparison study: implications for experimental design in AR5. Submitted.

11

12 Ramaswamy, V., O. Boucher, J. Haigh, D. Hauglustaine, J. Haywood, G. Myhre, T.

13 Nakajima, G.Y. Shi, S. Solomon, R. Betts, R. Charlson, C. Chuang, J.S. Daniel, A.

14 Del Genio, R. van Dorland, J. Feichter, J. Fuglestvedt, P.M. de F. Forster, S.J. Ghan,

15 A. Jones, J.T. Kiehl, D. Koch, C. Land, J. Lean, U. Lohmann, K. Minschwaner, J.E.

16 Penner, D.L. Roberts, H. Rodhe, G.J. Roelofs, L.D. Rotstayn, T.L. Schneider, U.

17 Schumann, S.E. Schwartz, M.D. Schwarzkopf, K.P. Shine, S. Smith, D.S. Stevenson,

18 F. Stordal, I. Tegen, and Y. Zhang, 2001: Radiative forcing of climate change.

19 *Climate Change 2001: The scientific basis. Contribution of working group I to the*

20 *third assessment report of the intergovernmental panel on climate change.* J.T.

21 Houghton, Y. Ding, D.J. Griggs, M. Noguer, P.J. van der Linden, X. Dai, K.

22 Maskell, and C.A. Johnson, Eds., Cambridge University Press, Cambridge, United

23 Kingdom and New York, NY, USA, 349-416.

24

1 Ramankutty, N. and J.A. Foley, 1999: Estimating historical changes in global land-  
2 cover: croplands from 1700 to 1992. *Glob. Biogeochem. Cycl.*, **13**, 997-1027.  
3

4 Rayner, N.A., D.E. Parker, E.B. Horton, C.K. Folland, L.V. Alexander and P. Frich,  
5 2000: The HadISST1 Global Sea-Ice and Sea Surface Temperature Dataset, 1871–  
6 1999. *Hadley Center Technical Note 17*.  
7

8 Rayner, N.A., D.E. Parker, E.B. Horton, C.K. Folland, L.V. Alexander, D. Rowell,  
9 E.C. Kent and A. Kaplan, 2003: Global analyses of sea surface temperature, sea ice,  
10 and night marine air temperature since the late nineteenth century. *J Geophys Res.*,  
11 **108**, 4407. doi: 10.1029/2002JD002670  
12

13 Stott, P.A., J.F.B. Mitchell, M.R. Allen, T. L. Delworth, J.M.Gregory, G.A. Meehl  
14 and B.D. Santer, 2006: Observational constraints on past attributable warming and  
15 predictions of future global warming. *J. Clim.*, **19**, 3055–3069.  
16

17 Tans, P., 2009: Earth System Research Laboratory, National Oceanic and  
18 Atmospheric Administration, Global Monitoring Division (NOAA/ESRL),  
19 <http://www.esrl.noaa.gov/gmd/ccgg/trends>, accessed 20 February 2009.  
20

21 Tung, K. K., J. Zhou, and C. D. Camp, 2008: Constraining model transient climate  
22 response using independent observations of solar-cycle forcing and response,  
23 *Geophys. Res. Lett.*, **35**, L17707, doi:10.1029/2008GL034240.  
24

1 Van den Hurk, B.J.J.M., P. Viterbo, A.C.M. Beljaars and A.K. Betts, 2000: Offline  
2 validation of the ERA40 surface scheme. *ECMWF TechMemo* **295**; see  
3 <http://www.ecmwf.int/publications/library/ecpublications/pdf/tm/001-300/tm295.pdf>  
4

5 Van der Molen, M.K., A.J. Dolman, M.J. Waterloo and L.A. Bruijnzeel, 2006:  
6 Climate is affected more by maritime than by continental land use change: a multiple  
7 scale analysis. *Glob. Plan. Change*, **54**, (1-2), 128-149, doi:  
8 10.1016/j.gloplacha.2006.05.005.  
9

10 Van Dorland, R., 1999: Radiation and Climate From Radiative Transfer Modelling to  
11 Global Temperature Response. PhD thesis, Utrecht University, the Netherlands, 147  
12 pp. ISBN 90-646-4032-7.  
13

14 Zhang, H., A. Henderson-Sellers and K. McGuffie, 1996a: Impacts of tropical  
15 deforestation. Part I: Process analysis of local climatic change. *J. Clim.*, **9**, 1497-1517.  
16

17 Zhang, H., K. McGuffie and A. Henderson-Sellers, 1996b: Impacts of tropical  
18 deforestation. Part II: The role of large-scale dynamics. *J. Clim.*, **9**, 2498-2521.  
19

20 Zhao, M., A.J. Pitman and T. Chase, 2001: The impact of land cover change on the  
21 atmospheric circulation. *Clim. Dyn.*, **17**, 467-477.

1 **Tables**

2

3 Table 1. Land cover distribution in 1750 (the reference year for radiative forcing),  
4 1870 (the ‘pre-industrial’ year in our simulations) and 1992 (the ‘present-day’ year in  
5 our simulations).

surface type	albedo	surface fraction A.D.		
		1750	1870	1992
ocean	0.07	0.72	0.72	0.72
land		0.28	0.28	0.28
low vegetation	0.20	0.09	0.10	0.12
high vegetation	0.13	0.13	0.12	0.10
bare ground	0.25	0.03	0.03	0.03
6 ice	0.50	0.03	0.03	0.03

1 Table 2. Radiative-Convective Model (RCM) calculations of the radiative forcing in  
 2 1750, 1870 and 1992 due to the change in land cover and albedo and due to the  
 3 increasing CO<sub>2</sub> concentrations. ‘RF’ is short for ‘Radiative Forcing’. The radiation  
 4 values apply to the tropopause level.

	year (A.D.)			change
RF due to land cover change	1750	1870	1992	1870-1992
clear sky albedo (-)	0.1079	0.1087	0.1102	
net short wave radiation (W m <sup>-2</sup> )	219.334	219.230	219.036	
radiative forcing (W m <sup>-2</sup> )	0.000	-0.104	-0.298	-0.19
surface temperature (K)	287.762	287.699	287.581	-0.12
RF due to CO <sub>2</sub> concentration change				
CO <sub>2</sub> concentration (ppm)	280	288	356	
net long wave radiation (W m <sup>-2</sup> )	-219.334	-219.201	-218.149	
radiative forcing (W m <sup>-2</sup> )	0.000	0.133	1.185	1.05
surface temperature (K)	287.762	287.845	288.479	0.63

5

1 Table 3. Comparison of the radiative forcing estimated with the RCM approach  
 2 (section 2 a) with the change in net radiation (including feedbacks) in the EC-Earth  
 3 climate model at the top of the atmosphere due to land cover change and/or increasing  
 4 CO<sub>2</sub> concentrations. The values represent the change in net radiation with respect to  
 5 1870 in W m<sup>-2</sup>. The characters in brackets refer to the type of simulation.

		increasing CO <sub>2</sub> concentration		
year		1870	1992	
increasing deforestation 	1870 RCM	(r) 0	(c) +1.05	
	EC-Earth	(r) 0	(c) +1.51	
	1992 RCM	(v) -0.19	(vc) +0.86	
	EC-Earth	(v) -0.20	(vc) +1.33	

6

1 Table 4. Feedback analysis using the RCM and EC-Earth estimates of change in  
2 radiation components, temperature and climate sensitivity to both land cover change  
3 (LCC) and CO<sub>2</sub> concentration change. The first two columns give the shortwave and  
4 long wave radiative forcings, the second two columns give the shortwave and long  
5 wave feedback (defined as the total change in net shortwave and long wave radiation  
6 minus the radiative forcing). The numbers represent the average feedback ( $\pm$  standard  
7 deviation) of (v-r) and (vc-c) in the case of LCC, and the average of (c-r) and (vc-v) in  
8 the case of CO<sub>2</sub> concentration change; In the case of the combined LCC and CO<sub>2</sub>  
9 concentration change, there is only one realization (vc-r). In the same way, the next  
10 columns give the change in net (all wave) radiation, surface temperature, climate  
11 sensitivity and total cloud fraction. The upper part gives the results on a global scale,  
12 and the lower part for the land only.

globally	radiative forcing		feedback		net dR <sub>n</sub> W m <sup>2</sup>	dT 2 m °C	$\lambda$ °C/(W m <sup>2</sup> )	df <sub>clouds</sub> %
	dR <sub>n,SW</sub> W m <sup>2</sup>	dR <sub>n,LW</sub> W m <sup>2</sup>	dR <sub>n,SW</sub> W m <sup>2</sup>	dR <sub>n,LW</sub> W m <sup>2</sup>				
LCC	-0.19	0	-0.07 ( $\pm$ 0.04)	0.07 ( $\pm$ 0.01)	-0.19 ( $\pm$ 0.02)	-0.04 ( $\pm$ 0.00)	0.22 ( $\pm$ 0.00)	0.02 ( $\pm$ 0.03)
CO <sub>2</sub>	0	1.05	0.75 ( $\pm$ 0.04)	-0.28 ( $\pm$ 0.01)	1.52 ( $\pm$ 0.02)	0.51 ( $\pm$ 0.00)	0.49 ( $\pm$ 0.00)	-0.50 ( $\pm$ 0.03)
LCC + CO <sub>2</sub>	-0.19	1.05	0.67	-0.20	1.33	0.47 ( $\pm$ 0.47)	0.55	-0.48
land only								
LCC	-0.56	0	-0.21 ( $\pm$ 0.07)	0.09 ( $\pm$ 0.05)	-0.70 ( $\pm$ 0.02)	-0.12 ( $\pm$ 0.00)	0.21 ( $\pm$ 0.00)	0.04 ( $\pm$ 0.09)
CO <sub>2</sub>	0	1.05	0.38 ( $\pm$ 0.07)	-0.27 ( $\pm$ 0.04)	1.16 ( $\pm$ 0.03)	0.66 ( $\pm$ 0.00)	0.62 ( $\pm$ 0.00)	-0.28 ( $\pm$ 0.09)
LCC + CO <sub>2</sub>	-0.56	1.05	0.17	-0.19	0.47	0.54 ( $\pm$ 0.54)	1.10	-0.24

13

1 Table 5. Analysis of linear additivity of the experiments where land cover (v-c) and  
 2 CO<sub>2</sub> concentration (c-r) were changed independently with respect to the experiment  
 3 where both were changed simultaneously (vc-r). The ‘slope’ represents a linear least  
 4 square regression coefficient in which the X data are the changes in (vc-r) and the Y  
 5 data are the sum of changes in (v-r) and (c-r). The upper part represents the analysis  
 6 where all grid points over the globe are used, whereas the lower part represents the  
 7 analysis where only grid points are used with more than 20% change in land cover.

selection	R <sub>net,SW</sub> sfc W m <sup>-2</sup>	R <sub>net,LW</sub> sfc W m <sup>-2</sup>	R <sub>net</sub> sfc W m <sup>-2</sup>	R <sub>net,SW</sub> toa W m <sup>-2</sup>	R <sub>net,LW</sub> toa W m <sup>-2</sup>	R <sub>net</sub> toa W m <sup>-2</sup>	H sfc W m <sup>-2</sup>	LE sfc W m <sup>-2</sup>	cloud cover %	precip. mm yr <sup>-1</sup>	T 2 m °C	θ top dm <sup>3</sup> m <sup>-3</sup>
global												
RMSE	1.00	0.70	0.60	0.80	0.60	0.50	0.80	1.10	0.60	40.50	0.10	1.60
r <sup>2</sup>	0.89	0.72	0.93	0.90	0.84	0.94	0.89	0.86	0.75	0.75	0.93	0.57
slope	0.99	0.90	1.01	1.00	1.05	1.00	0.95	0.99	0.98	1.01	1.03	0.85
Δf <sub>high</sub>   > 0.20												
RMSE	1.20	0.90	0.60	1.00	0.70	0.60	1.30	1.30	0.70	37.60	0.10	2.70
r <sup>2</sup>	0.94	0.79	0.98	0.95	0.78	0.98	0.91	0.74	0.72	0.81	0.94	0.71
slope	1.02	0.96	1.04	1.02	1.10	1.01	0.99	0.97	1.06	1.00	0.92	0.98

8

1 **Figure Captions**

2 Figure 1. Change in SST (left) and SIC (right) between the present-day and pre-  
3 industrial experiments.

4

5 Figure 2. Change in the fraction of high vegetation (present-day – pre-industrial) and  
6 the resulting change in surface albedo.

7

8 Figure 3. Climate sensitivity parameters ( $^{\circ}\text{C} / \text{W m}^{-2}$ ) for land cover change and  $\text{CO}_2$   
9 concentration change. The climate sensitivity for land cover change is determined at  
10 historic (v-r) and present day  $\text{CO}_2$  concentration (vc-c), and the climate sensitivity for  
11  $\text{CO}_2$  change is determined at historic (c-r) and present day land cover (vc-v). The  
12 climate sensitivities are determined on a global basis as well as for land area alone.

13

14 Figure 4. The change in high (top) and low (middle) and total (bottom) cloud cover  
15 fraction as a result of land cover change (left) and  $\text{CO}_2$  concentration change (right).

16

17 Figure 5. The change in TOA net shortwave radiation (top left), net long wave  
18 radiation (top right), net all wave radiation (bottom left) and total cloud cover (bottom  
19 right) as a function of the change in albedo in the EC-Earth simulation with only  
20 vegetation changes (v) with respect to the reference simulation (r). The thin lines  
21 represent the direct shortwave radiative effect of albedo change and the deviation  
22 from the straight line indicates the impact of feedbacks. Results are shown for the  
23 Northern Hemispheric mid-latitudes ( $45\text{-}60^{\circ}$ ) and tropical latitudes ( $-15 - 15^{\circ}$ ).

24

1 Fig. 6. The change in surface temperature as a function of change in albedo in the EC-  
2 Earth simulation with only vegetation changes (v) with respect to the reference  
3 simulation (r).

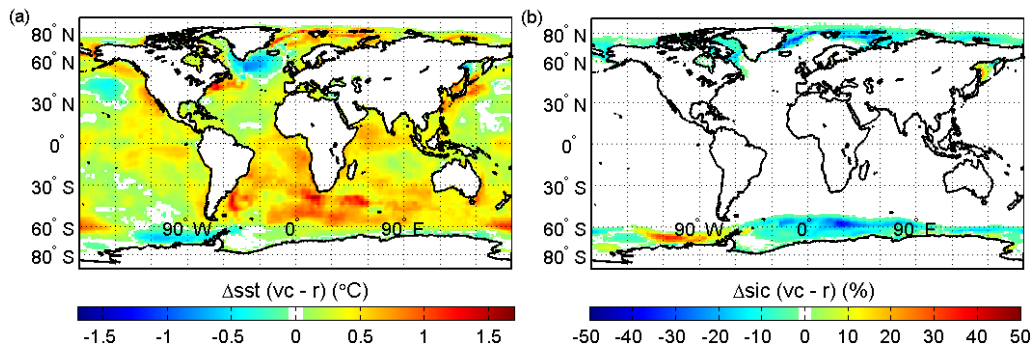
4

5 Fig. 7. The change in surface sensible (left) and latent (right) heat flux as a function of  
6 the change in albedo in the EC-Earth simulation with only vegetation changes (v) with  
7 respect to the reference simulation (r).

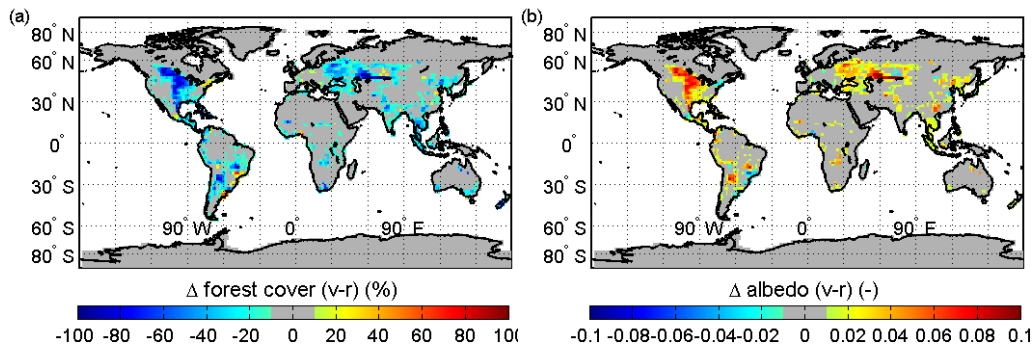
8

9 Fig. 8. The change in net long wave (left) and shortwave (right) radiation at the  
10 surface (top) and at the top of the atmosphere (bottom) as a function of latitude in the  
11 EC-Earth simulation with only increased CO<sub>2</sub> concentration (c) with respect to the  
12 reference simulation (r). The shaded areas represent the variation between the 1<sup>st</sup> and  
13 99<sup>th</sup> percentiles and the solid lines represent the mean.

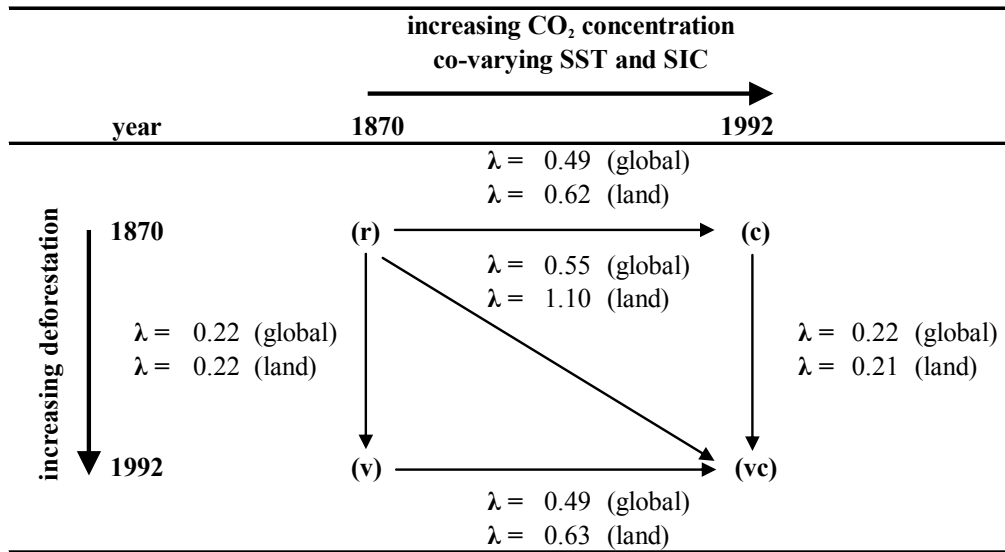
1 **Figures**



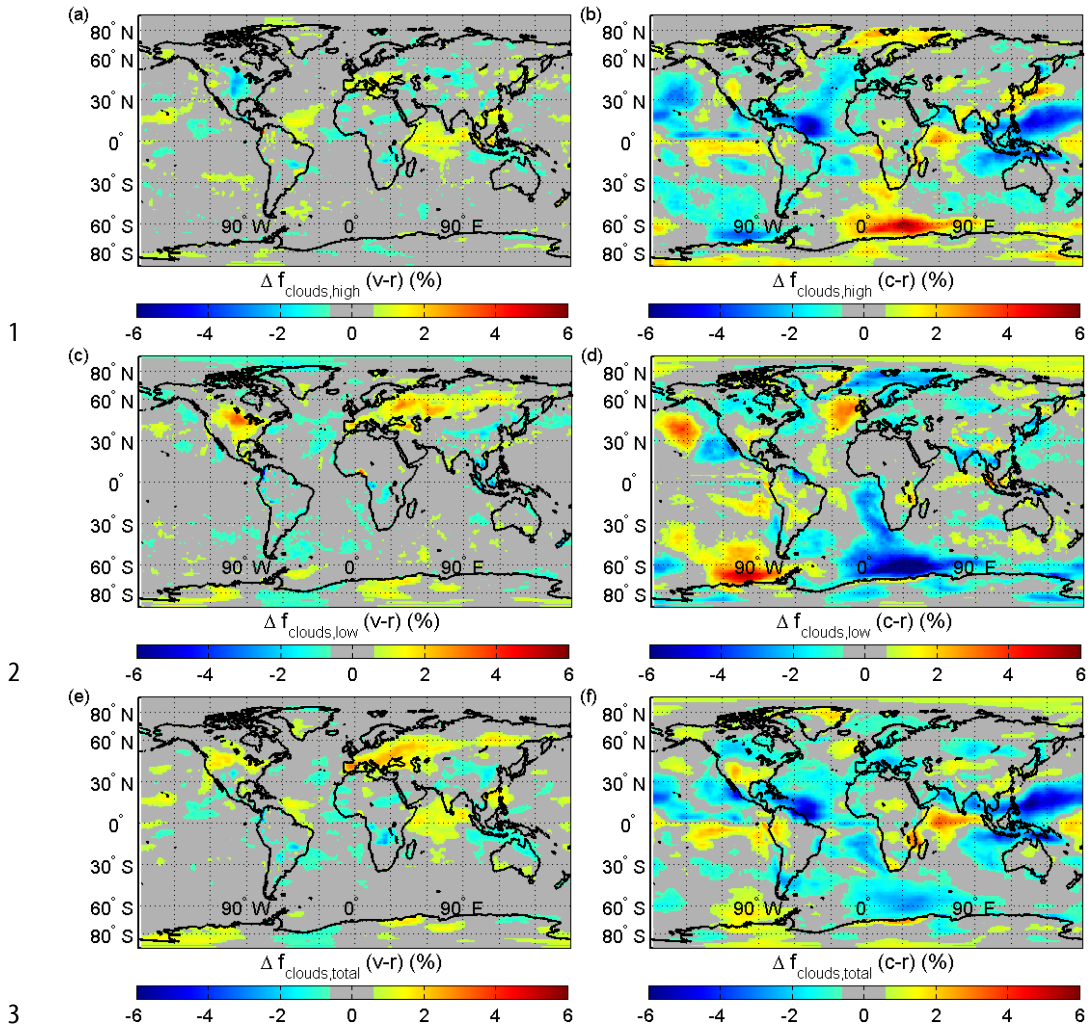
3 Figure 1. Change in SST (a) and SIC (b) between the present-day and pre-industrial  
4 experiments.



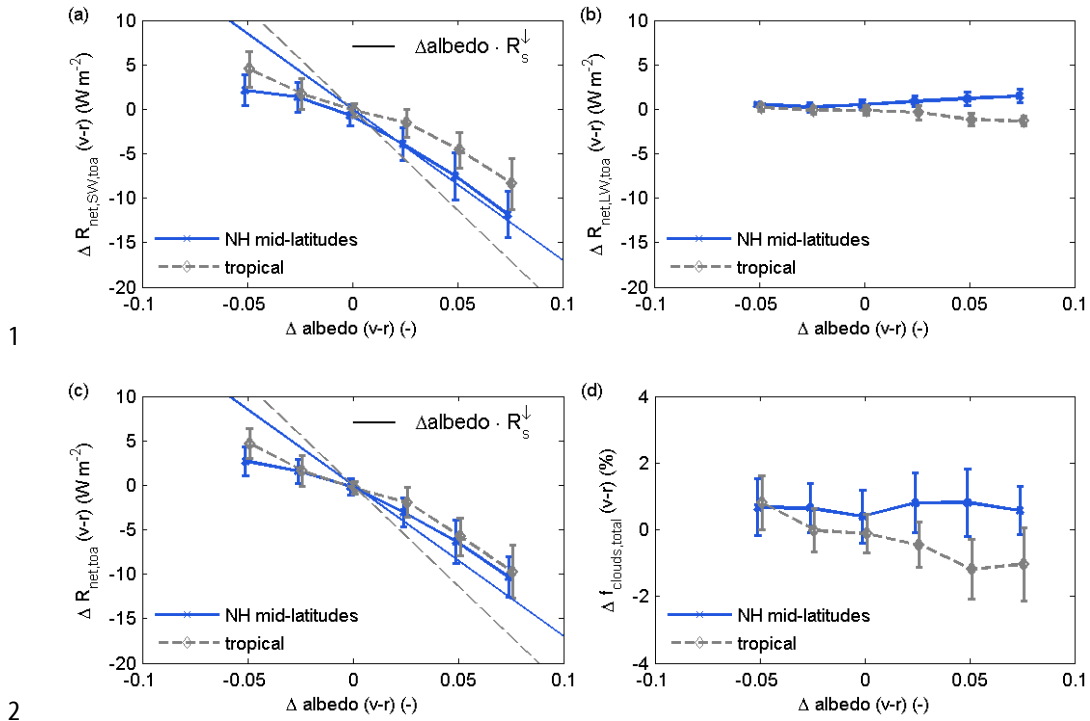
8 Figure 2. Change in (a) the fraction of high vegetation (present-day – pre-industrial)  
9 and (b) the resulting change in surface albedo.



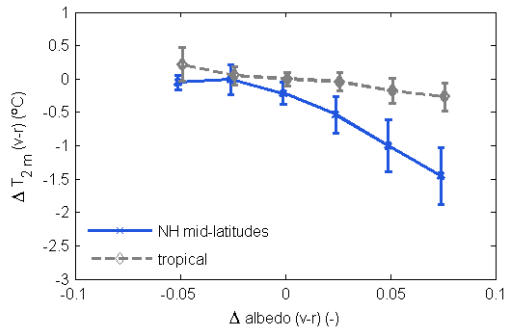
1  
 2 Figure 3. Climate sensitivity parameters ( $^{\circ}\text{C} / \text{W m}^{-2}$ ) for land cover change and CO<sub>2</sub>  
 3 concentration change. The climate sensitivity for land cover change is determined at  
 4 historic (v-r) and present day CO<sub>2</sub> concentration (vc-c), and the climate sensitivity for  
 5 CO<sub>2</sub> change is determined at historic (c-r) and present day land cover (vc-v). The  
 6 climate sensitivities are determined on a global basis as well as for land area alone.



4 Figure 4. The change in high (top) and low (middle) and total (bottom) cloud cover  
 5 fraction as a result of land cover change (left) and CO<sub>2</sub> concentration change (right).



1  
2  
3 Figure 5. The change in TOA (a) net shortwave radiation, (b) net long wave  
4 radiation, (c) net all wave radiation and (d) total cloud cover as a function of the  
5 change in albedo in the EC-Earth simulation with only vegetation changes (v) with  
6 respect to the reference simulation (r). The thin lines represent the direct shortwave  
7 radiative effect of albedo change and the deviation from the straight line indicates the  
8 impact of feedbacks. Results are shown for the Northern Hemispheric mid-latitudes  
9 (45-60°) and tropical latitudes (-15 - 15°).



1

2 Fig. 6. The change in surface temperature as a function of change in albedo in the EC-

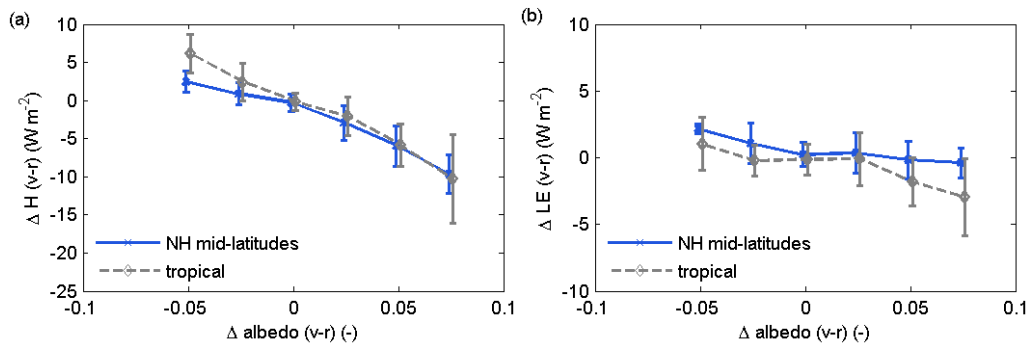
3 Earth simulation with only vegetation changes (v) with respect to the reference

4 simulation (r).

5

6

7

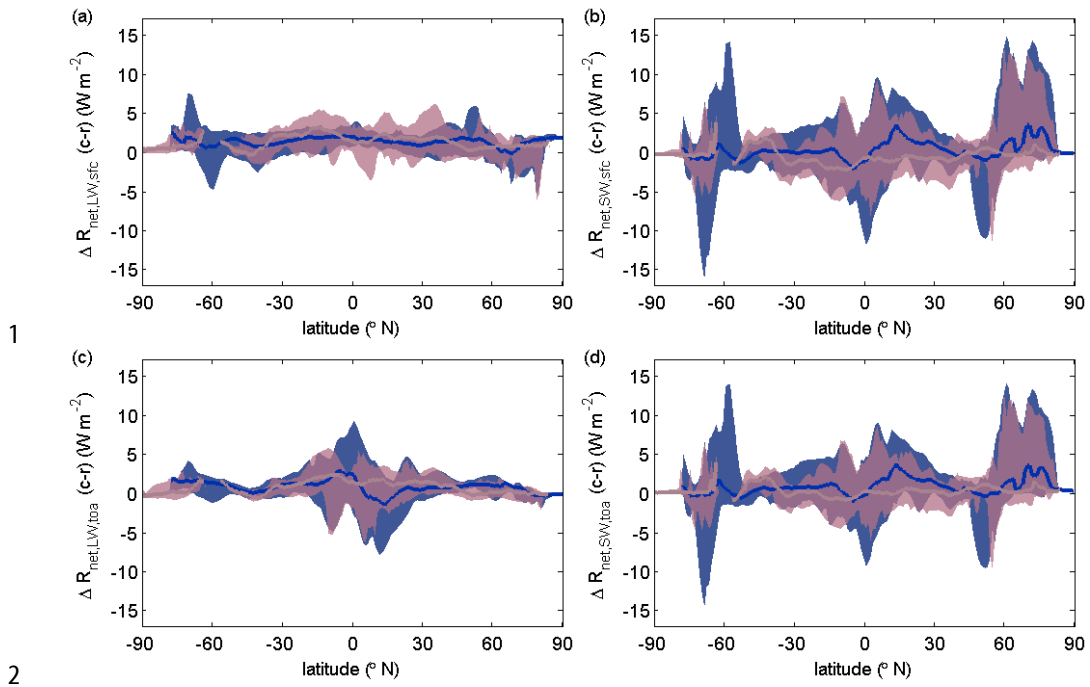


8

9 Fig. 7. The change in surface sensible (a) and latent (b) heat flux as a function of the

10 change in albedo in the EC-Earth simulation with only vegetation changes (v) with

11 respect to the reference simulation (r).



1  
 2  
 3 Fig. 8. The change in net long wave (left) and shortwave (right) radiation at the  
 4 surface (top) and at the top of the atmosphere (bottom) as a function of latitude in the  
 5 EC-Earth simulation with only increased CO<sub>2</sub> concentration (c) with respect to the  
 6 reference simulation (r). The shaded areas represent the variation between the 1<sup>st</sup> and  
 7 99<sup>th</sup> percentiles and the solid lines represent the mean.